Analysis of the Singlet−Triplet Splitting Computed by the Density Functional Theory−Broken−Symmetry Method: Is It an Exchange Coupling Constant?

ARTICLE *in* INORGANIC CHEMISTRY · JUNE 2011

Impact Factor: 4.76 · DOI: 10.1021/ic200198f · Source: PubMed

Inorganic Chemistry

ARTICLE

pubs.acs.org/IC

Analysis of the Singlet−Triplet Splitting Computed by the Density Functional Theory−Broken-Symmetry Method: Is It an Exchange Coupling Constant?

Nicolas Onofrio* and Jean-Marie Mouesca*

Laboratoire de Résonances Magnétiques, Service de Chimie Inorganique et Biologique UMR-E 3 CEA-UJF, Institut de Nanosciences et Cryogénie, CEA-Grenoble, 17 rue des Martyrs, 38054 Grenoble Cedex 9, France

Supporting Information

ABSTRACT: We derive an analytical expression of the density functional theory (DFT)−broken-symmetry (BS) estimation J^{BS} of the singlet−triplet gap at the "3 sites−4 electrons" level, that is, two $S = {}^1/_2$ metallic sites + one diamagnetic bridge orbital. As originally designed by Noodleman and Davidson (*Chem. Phys.* **1986**, *109*, 131), J^{BS} contains the residual ferromagnetic contribution, single ligand-to-metal and metal-to-metal charge-transfer terms, but no double ligand-to-metal charge-transfer terms or intra/interligand spin-polarization terms. As revealed by the present analysis, the triplet and BS states computed by DFT differ, not only perturbatively (as expected) because of the various physical mechanisms involved (i.e., differential charge-transfer terms) but mainly because of a spurious and unphysical symmetry breaking of the bridge orbitals in the BS state. We examine the consequences of such a difference by deriving two analytical expressions of the exchange coupling constant, one from the BS orbitals designed to match J^{BS} and another one from triplet orbitals only. Following and extending on the first paper in the series (*J. Phys. Chem. A* **2010**, *114*, 6149), we propose a simple procedure to extract appropriate parameters filling in our analytical expressions. Moreover, we derive the equivalent "3 sites−4 electrons" exchange coupling constant in the configuration-interaction approach, J^{CI}, for the purpose of comparison. These analytical expressions have been applied to various copper dimers and compared to experimental values.

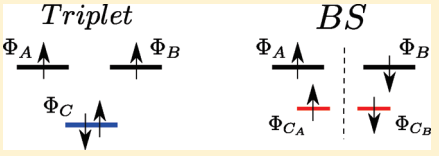

INTRODUCTION

Density functional theory (DFT) combined with the broken-symmetry (BS) method is today widely used in the field of molecular magnetism for the calculation of exchange coupling constants. The BS method, as it applies to the study of the exchange interaction within spin-coupled transition-metal dimers, was first proposed by Noodleman and co-workers[1−3] (see also subsequent reformulations by Hart and co-workers[4] as well as by Ciofini and Daul[5]). It consists of evaluating the magnetic exchange coupling constant J from the energy difference between high-spin (HS; of spin S_{max}) and BS ($M_S = 0$) configurations constructed from a set of nonorthogonal valence-bond (NO-VB) magnetic orbitals $\{\Phi_A, \Phi_B\}$ with the overlap $S = \langle\Phi_A|\Phi_B\rangle$. Only homodimers will be considered in this paper, with, moreover, $H_{Heis} = -JS_A \cdot S_B$. In the so-called weak interaction limit ($S^2 \ll 1$), $J^{BS} = 2(E_{BS} - E_{HS})/{S_{max}}^2$ (but see, for example, Noodleman and Case[3] and Yamaguchi et al.,[6] where this restriction is removed). The BS wave function[7−9] itself is not a pure spin state but a state of mixed spin and spatial (orbital) broken symmetry, where the α and β magnetic electrons are localized on the left and right metal sites, respectively.

In transition-metal dimer complexes, the magnetic interaction can be monitored through an appropriate choice of bridging ligands. Numerous DFT−BS studies aim, therefore, at rationalizing the sign and strength of the exchange coupling for various bridges by drawing magnetostructural correlations in order to design new magnetic systems of targeted properties, especially ferromagnetism[10−15] (and references cited therein). Consequently, the DFT−BS method turns out to be a powerful tool to predict and rationalize experimental trends. In addition, some attention has been given to the DFT−BS analysis of polyspin systems, which gives some crucial point of comparison to the experiment.[16,17] This is done by reducing the above phenomenological Heisenberg Hamiltonian H_{Heis} to its diagonal elements, i.e., to an Ising-type Hamiltonian $H_{Ising} = -\Sigma_{i,j}J_{ij}M_{S_i}M_{S_j}$, where the spins of the building blocks (monomers) are kept fixed. Beyond the intramolecular exchange interaction, some studies have reported very interesting results concerning intermolecular interactions.[18] In summary, the choice of the DFT−BS method rests on both its conceptual simplicity and its low computational cost, which makes it a good investigative tool for calculation of the electronic structures and magnetic properties of large systems.

Unfortunately, the DFT−BS method remains semiquantitative because it suffers from a series of drawbacks, both conceptual (BS) and practical (DFT), some of which have already been discussed in the literature:[2,19]

(i) Conceptually, the BS wave function was developed on the basis of an initial covalent ground-state determinant

Received: January 28, 2011
Published: May 27, 2011

further refined by the addition of determinants formed by single excitations with respect to it. This procedure yields the necessary metal−metal and ligand−metal charge-transfer terms (MMCT and LMCT, respectively) resulting in antiferromagnetic contributions to J^{BS}. However, no double ligand-to-metal charge transfer (DCT) and no intra/interligand spin polarization are taken into account in spite of their mechanistic importance.[20−26] The absence of the two latter mechanisms has been recognized as *almost certainly the most serious omission in the BS method*.[2]

(ii) Practically, the DFT−BS method suffers from spin contamination because it deals with unrestricted determinants rather than with pure spin states. This problem is usually limited in the HS state, and for copper(II) dimers, the S^2 operator yields eigenvalues very close to the expected 2. By contrast, the corresponding BS state is by construction spin-contaminated, although in the weak limit, it is ideally a controlled mixture of all $M_S = 0$ components of pure spin states ranging from $S_{min} = 0$ to S_{max} and weighed by Clebsch−Gordan coefficients. Again, for copper(II) dimers, the S^2 operator typically yields values close to 1, intermediate between 0 (pure singlet) and 2 (pure triplet). However, this idealization itself rests on the approximation that the monomeric spin-bearing building blocks do not change by the spin-flip procedure, leading from HS to BS.

(iii) The computed values of J^{BS} depend on the choice of the exchange-correlation (XC) potential. In that regard, hybrid potentials mixing into the local DFT exchange some percentage of nonlocal Hartree−Fock (HF) exchange have been favored over the last years in order to correct for the (local) DFT tendency to overestimate magnetic orbital delocalization. Typically, combining a 20% HF contribution to the XC potential (B3LYP) and an empirical reduction of the resulting exchange coupling constant by a factor 2 seems to give values close to the experimental ones. It is (in our view) still a matter of debate[27−29] whether this empirical factor 2 universally corrects for the so-called self-interaction errors (SIEs) inherent to the conventional DFT computation of exchange coupling constants (see more about this in the Conclusion section).

(iv) Finally, beyond magnetostructural correlations and attempts to rationalize the BS method by developing the DFT−BS magnetic orbital in terms of atomic ones, there is, to our knowledge, no analytical expression of J^{BS} beyond the "2 sites−2 electrons" level,[7,30−33] for which it assumes the closed form[1] $J^{BS} = 2j^{MO} - US^2$, where $2j^{MO}$ is the residual ferromagnetic bielectronic exchange integral defined for orthogonalized magnetic orbitals and U is the energy difference between the ionic and covalent configurations.

By contrast, multideterminant ab initio methods give very good agreement with the experiment. These methods deal with the exact electronic Hamiltonian, and all relevant physical effects can, in principle, be incorporated in the treatment. This yields an analysis of the various contributions to the exchange coupling constant at each order of perturbation.[26,34,35] In that regard, the difference-dedicated configuration interaction (DDCI)[36] method has been fully tested for the calculation of exchange coupling constants over a significant range of magnetic materials. In the case of copper dimers, this method consists of a direct perturbation treatment of the sole determinants contributing to the singlet−triplet energy difference. This allows one to reduce the number of states actually involved in the numerical calculations. Nevertheless, the computational cost of ab initio CI calculations is still high, in particular for systems involving several metallic centers with local spins $S_i > {}^1/_2$. Moreover, some convergence problems appear for the treatment of large systems, although, recently, alternative strategies have been proposed to reduce the size of the CI matrices[37] or the number of matrix elements to be computed.[19]

In this work, we aim to establish a formal link between the DFT−BS and ab initio CI methods by developing two analytical expressions of the exchange coupling constant at the same level of approximation, one aiming at reproducing J^{BS} and the other one mimicking the equivalent J^{CI} constant. We will mostly limit our derivations to "3 sites−4 electrons", with one unpaired electron for each of the two paramagnetic sites and two electrons for the third diamagnetic bridging site linking them. In order to reproduce J^{BS}, we will explicitly take into account the following physical mechanisms at the origin of the DFT−BS singlet−triplet gap: the ferromagnetic potential exchange and the MMCT and LMCT terms. We will show how one of the two analytical expressions, supplied with parameters extracted from the DFT (HS and BS) states, matches J^{BS} for copper(II) dimers. We will have verified numerically that, as anticipated by Noodleman and Davidson,[2] the BS procedure as modeled within our approach does not include either double excitation nor intra/interligand spin-polarization contributions.

In the course of our investigations, we stumbled onto another feature of the BS state as embodied in DFT calculations. By definition of the exchange mechanism, the same initial orbital basis is assumed for the initial construction of both triplet and singlet wave functions, and upon computation of their energy difference, they should finally differ only as a result of the physical mechanisms involved (i.e., charge-transfer terms at various orders of perturbation). The BS formalism was, of course, originally developed with such a conceptual background. In practice though, such is not the case when DFT−HS/BS calculations were performed. We will show how the shape of the (doubly occupied) bridge molecular orbitals (MOs) is artificially altered when their symmetry is broken from HS to BS. This will have a strong impact on the analytical formulation of the exchange coupling constant not visible at the "2 sites−2 electrons" level but manifested at the "3 sites−4 electrons" level. Hence, the thought-provoking title of the present paper: is J^{BS} really an exchange coupling constant?

THEORETICAL FORMALISM

In order to clarify the presentation, we derive two new analytical expressions of J within the simple "3 sites−4 electrons" model (i.e., two $S = {}^1/_2$ Cu^{II} ions and one diamagnetic bridge orbital). We will only consider one of the two possible symmetries of the bridge orbitals, the one selected by the *gerade* triplet singly occupied molecular orbital (SOMO). In the Appendix, we will briefly extend this first derivation by including both bridge orbitals' symmetries (*gerade* and *ungerade*). In order to keep the derivation as light as possible, we will only report in the main text of the paper the key equations. Some of the necessary mathematical ingredients and key steps of the full derivation are detailed in section A in the Supporting Information. Finally, all concepts, as well as analysis of

the DFT (HS and BS) output files, are first performed within the NO-VB framework, before being recast into an orthogonalized atomic picture for the sake of mathematical simplicity. All formal derivations have been performed with both the computer algebra system *Maxima 5.20.1* package (2009; http://maxima.sourceforge.net) and homemade *Python* (2.6.5) codes.

Magnetic Orbitals. *NO-VB Description of a Monomer within the BS State.* On one side of the BS state, the construction of the NO-VB magnetic orbitals[38−41] starts with the interaction matrix between the atomic metallic A (i.e., d_A) and bridge C (i.e., p_z) orbitals where z stands for the Cu−Cu axis (all nonorthogonal quantities with uppercase indices). The resulting (antibonding) magnetic Φ_A and (bonding) bridge Φ_{C_A} orbitals are given by (up to second order in $H_{(A,C)}/\Delta_{AC}$ and σ_{AC}):[42]

$$\Phi_A \approx \left(\frac{H_A}{\Delta_{AC}}\right)C + \left(1 - \frac{H_A}{\Delta_{AC}}\sigma_{AC} - \frac{{H_A}^2}{2{\Delta_{AC}}^2}\right)A \quad (1)$$

$$\Phi_{C_A} \approx \left(1 + \frac{H_C}{\Delta_{AC}}\sigma_{AC} - \frac{{H_C}^2}{2{\Delta_{AC}}^2}\right)C - \left(\frac{H_C}{\Delta_{AC}}\right)A \quad (2)$$

where $\Delta_{AC} = E_A - E_C$ with $E_A = \langle A|h^{\text{eff}}|A\rangle$ and $E_C = \langle C|h^{\text{eff}}|C\rangle$. Moreover, $h_{AC} = \langle A|h^{\text{eff}}|C\rangle$ and $\sigma_{AC} = \langle A|C\rangle$, from which $H_A = h_{AC} - E_A\sigma_{AC}$ and $H_C = h_{AC} - E_C\sigma_{AC}$. Finally, the effective Hamiltonian h^{eff} is the Kohn−Sham (KS) monoelectronic operator for the optimized BS state (more about this below). We showed in the first paper in the series[9] how to carefully reconstruct the localized VB magnetic orbitals $\{\Phi_A, \Phi_B\}$ from the corresponding partially delocalized DFT−BS orbitals $\{\Phi_A^{\text{BS}}, \Phi_B^{\text{BS}}\}$, assuming the following Coulson−Fisher linear relationship: $\Phi_A^{\text{BS}} = \lambda\Phi_A + \mu\Phi_B$ with $\overline{S} = \langle\Phi_A^{\text{BS}}|\Phi_B^{\text{BS}}\rangle = S + 2\lambda\mu(1 - S^2)$. The quantity $\overline{S}$ will be computed numerically (cf. the Methodology section). The ratio μ/λ is derived from that of the copper d orbitals in Φ_A^{BS}. The VB overlap $S = \langle\Phi_A|\Phi_B\rangle$ is then computed from $\overline{S}$ and μ/λ. The whole procedure finally yields λ and μ. Consequently, in Noodleman's formulation of J^{BS}, the antiferromagnetic contribution, $-US^2$, is replaced by $-U\overline{S}^2$. Notice that no analysis of the VB overlap S had been offered in terms of its atomic content in the first paper in the series. From the reconstructed NO-VB magnetic orbital $\Phi_A \approx c_C C + c_A A$ (+ other terms ...), one can extract the coefficients' ratio $c_C/c_A \approx H_A/\Delta_{AC}$ (to second order).

The nonorthogonal atomic orbitals $\{A, B, C\}$ in eqs 1 and 2 are recast in terms of orthogonalized atomic orbitals $\{a, b, c\}$:[39,41,43]

$$\begin{cases} A = \frac{1}{2}(\sqrt{1+\sigma_{AB}} + \sqrt{1-\sigma_{AB}})a + \frac{1}{2}(\sqrt{1+\sigma_{AB}} - \sqrt{1-\sigma_{AB}})b \\ B = \frac{1}{2}(\sqrt{1+\sigma_{AB}} - \sqrt{1-\sigma_{AB}})a + \frac{1}{2}(\sqrt{1+\sigma_{AB}} + \sqrt{1-\sigma_{AB}})b \\ C = \left(\sqrt{1 - \frac{2{\sigma_{AC}}^2}{1+\sigma_{AB}}}\right)c + \frac{\sigma_{AC}}{\sqrt{1+\sigma_{AB}}}a + \frac{\sigma_{AC}}{\sqrt{1+\sigma_{AB}}}b \end{cases} \quad (3)$$

with $\sigma_{AB} = \langle A|B\rangle$. It will be applied to both BS and triplet states in order to carefully compare at the same level of formulation computed energies and exchange coupling constants. Up to second order in σ_{AC} and the ratio h_{ac}/δ_{ac}, the same previous NO-VB orbitals are expressed as

$$\Phi_A \approx \left(\frac{h_{ac}}{\delta_{ac}}\right)c + \left(1 - \frac{{h_{ac}}^2}{2{\delta_{ac}}^2}\right)a + \left(\frac{\sigma_{AB}}{2} + \frac{h_{ac}\sigma_{AC}}{\delta_{ac}}\right)b \quad (4)$$

$$\Phi_{CA} \approx \left(1 - \frac{{\sigma_{AC}}^2}{2} - \frac{{h_{ac}}^2}{2{\delta_{ac}}^2}\right)c + \left(-\frac{h_{ac}}{\delta_{ac}}\right)a + (\sigma_{AC})b \quad (5)$$

where $\delta_{ac} = \langle a|h^{\text{eff}}|a\rangle - \langle c|h^{\text{eff}}|c\rangle$ and $h_{ac} = \langle a|h^{\text{eff}}|c\rangle$. From the $\{A, B, C\} \leftrightarrow \{a, b, c\}$ correspondence (cf. eq 3), it turns out that $c_C/c_A \approx H_A/\Delta_{AC} \approx h_{ac}/\delta_{ac}$ (to second order). Finally

$$\overline{S} = S + 2\lambda\mu(1 - S^2) \approx \sigma_{AB} + 2\mu + \frac{2h_{ac}\sigma_{AC}}{\delta_{ac}} + \frac{{h_{ac}}^2}{{\delta_{ac}}^2} \quad (6)$$

In this "3 sites−4 electrons" formulation, $\overline{S}$ is decomposed into both intersite delocalization terms (direct overlap σ_{AB} and ionic−covalent mixing coefficient 2μ) and additional bridge-only terms, exhibiting site-specific (here metal and bridge) atomic details not explicit at the simpler "2 sites−2 electrons" level.

VB Description of the Triplet State. The same second-order procedure can be used for the VB description of the triplet state. The construction of the VB magnetic orbitals from the triplet state starts with the interaction matrix between the symmetry-adapted atomic orbitals $(A \pm B)/\sqrt{2}$ and C yielding

$$\Phi_g \approx \left(\frac{\sqrt{2}H_A}{\Delta_{AC}}\right)C + \left(1 - \frac{\sigma_{AB}}{2} - \frac{H_A\sigma_{AC}}{\Delta_{AC}} - \frac{{H_A}^2}{{\Delta_{AC}}^2}\right)\frac{A+B}{\sqrt{2}} \quad (7)$$

$$\Phi_u \approx \frac{A-B}{\sqrt{2}} \quad (8)$$

$$\Phi_C \approx \left(1 + \frac{2H_C\sigma_{AC}}{\Delta_{AC}} - \frac{{H_C}^2}{{\Delta_{AC}}^2}\right)C - \left(\frac{\sqrt{2}H_C}{\Delta_{AC}}\right)\frac{A+B}{\sqrt{2}} \quad (9)$$

Using the orthogonalization procedure defined in eq 3 and up to second order in h_{ac}/δ_{ac}, the same previous NO-VB orbitals are now expressed as

$$\Phi_g = \left(\frac{\sqrt{2}h_{ac}}{\delta_{ac}}\right)c + \left(1 - \frac{{h_{ac}}^2}{{\delta_{ac}}^2}\right)\frac{a+b}{\sqrt{2}} \quad (10)$$

$$\Phi_u = \frac{a-b}{\sqrt{2}} \quad (11)$$

$$\Phi_C = \left(1 - \frac{{h_{ac}}^2}{{\delta_{ac}}^2}\right)c - \left(\frac{\sqrt{2}h_{ac}}{\delta_{ac}}\right)\frac{a+b}{\sqrt{2}} \quad (12)$$

By recombining (±) the two SOMOs (taking into account the overlap S), one recovers exactly $\{\Phi_A, \Phi_B\}$ (eq 4). The SOMOs' energy gap Δ_{gu} is given by

$$\Delta_{gu} \approx 2h_{ab} + \frac{2{h_{ac}}^2}{\delta_{ac}} \quad (13)$$

where $h_{ab} = \langle a|h^{\text{eff}}|b\rangle$. The triplet state Φ_C orbital (eq 12) is symmetrical in $a \leftrightarrow b$, whereas the BS Φ_{C_A} orbital is not (eq 5). Moreover, it can be verified that Φ_C is not equal to the normalized sum of Φ_{C_A} and Φ_{C_B}. In other words, a "3 sites−4 electrons" analysis of both the triplet and BS states reveals that the dimer cannot be seen as a simple linear superposition of the monomers from a DFT−BS point of view. Alternatively, the computation of the energies E_T and E_{BS} leading to $J^{\text{BS}} \approx 2(E_{BS} - E_T)$ is not performed with the *same* set of MOs (as far as the bridge is concerned). This difference between Φ_C and Φ_{C_A} occurs because, in the triplet state, Φ_C is orthogonal to *both* magnetic orbitals

dx.doi.org/10.1021/ic200198f |*Inorg. Chem.* 2011, 50, 5577–5586

$\{\Phi_A, \Phi_B\}$. whereas in the BS state, Φ_{C_A} is only orthogonal to Φ_A (respectively, Φ_{C_B} is orthogonal to Φ_B: see Figure 1; there is more about this in the Discussion section). As a consequence, the KS effective Hamiltonian h^{eff}, functional of the total density, is not exactly the same for both the T and BS states. In the next section devoted to the derivation of analytical exchange coupling constants' expressions, we will remedy these issues by constructing singlet and triplet states from two alternative sets of MOs (the so-called "top-down" approach, going down from molecular to atomic details). Before that, and for comparison purposes, we first formulate a more classic "bottom-up" approach, constructing triplet and singlet states from the previously defined set of mutually orthogonalized $\{a, b, c\}$ atomic orbitals.

Exchange Coupling Constants. *Bottom-Up Derivation of J^{CI}.* On the basis of the determinants represented in Table 1, constructed from $\{a, b, c\}$, the full CI matrix for a singlet state $^1\Psi_{GS}$ is expressed in terms of the basic singlet states ($^1\Psi_{COV}$, $^1\Psi_{LMCT}$, $^1\Psi_{MMCT}$, $^1\Psi_{DCT}$) as

$$\begin{bmatrix} K_{ab} & -\sqrt{2}h_{ac} & 2h_{ab} & 0 \\ -\sqrt{2}h_{ac} & \delta_{ac} & \sqrt{2}h_{ac} & 2h_{ac} \\ 2h_{ab} & \sqrt{2}h_{ac} & U & 0 \\ 0 & 2h_{ac} & 0 & \Delta E_{DCT} \end{bmatrix} \tag{14}$$

where the bielectronic exchange integral $K_{ab} = \langle ab|1/r_{12}|ba\rangle$ is made explicit in the covalent singlet energy only and $\Delta E_{DCT} = E_{DCT} - E_{COV}$.

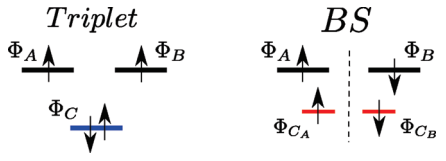

Figure 1. Schematic representation of both the triplet and BS magnetic and bridge orbitals.

Second-order perturbation theory yields the following ground-state singlet wave function:

$$^1\Psi_{GS} = \left(1 - \frac{h_{ac}^2}{\delta_{ac}^2}\right)^1\Psi_{COV} + \left(\frac{\sqrt{2}h_{ac}}{\delta_{ac}}\right)^1\Psi_{LMCT} - \frac{2}{U}\left(h_{ab} + \frac{h_{ac}^2}{\delta_{ac}}\right)^1\Psi_{MMCT} - \left(\frac{2\sqrt{2}h_{ac}^2}{\delta_{ac}\Delta E_{DCT}}\right)^1\Psi_{DCT} \tag{15}$$

At the level of this "bottom-up" approach, constructing $^1\Psi_{GS}$ from $\{a, b, c\}$ and resulting elementary singlets, we do not need to give explicit shapes to the magnetic and bridge orbitals. Likewise, the CI matrix for the triplet state $^3\Psi_{GS}$ can be expressed in terms of $^3\Psi_{COV}$ and $^3\Psi_{LMCT}$, formally identical with the first two terms in eq 15:

$$^3\Psi_{GS} = \left(1 - \frac{h_{ac}^2}{\delta_{ac}^2}\right)^3\Psi_{COV} + \left(\frac{\sqrt{2}h_{ac}}{\delta_{ac}}\right)^3\Psi_{LMCT} \tag{16}$$

Finally, from the singlet−triplet energy difference, we derive the following "3 sites−4 electrons" analytical expression of J^{CI} (cf. eq 13):

$$J^{CI} = 2K_{ab} - \frac{4}{U}\left(h_{ab} + \frac{h_{ac}^2}{\delta_{ac}}\right)^2 - \frac{8h_{ac}^4}{\delta_{ac}^2\Delta E_{DCT}} = 2K_{ab} - \frac{\Delta_{gu}^2}{U} - \frac{8h_{ac}^4}{\delta_{ac}^2\Delta E_{DCT}} \tag{17}$$

This atomic CI expression, including the last DCT term, is formally identical with that derived from orthogonal MOs in the

Table 1. Basic Singlet and Triplet Wave Functions and Schematic Representations of Their Contributing Determinants[a]

Basic singlet and triplet states	Schematic representations
$^1\Psi_{COV} = \frac{1}{\sqrt{2}}(\lvert a\bar{b}c\bar{c}\rvert + \lvert b\bar{a}c\bar{c}\rvert)$	$\lvert a\bar{b}c\bar{c}\rvert$ $\lvert b\bar{a}c\bar{c}\rvert$
$^3\Psi_{COV} = \frac{1}{\sqrt{2}}(\lvert a\bar{b}c\bar{c}\rvert - \lvert b\bar{a}c\bar{c}\rvert)$	
$^1\Psi_{MMCT_1} = \frac{1}{\sqrt{2}}(\lvert a\bar{a}c\bar{c}\rvert + \lvert b\bar{b}c\bar{c}\rvert)$	$\lvert a\bar{a}c\bar{c}\rvert$ $\lvert b\bar{b}c\bar{c}\rvert$
$^1\Psi_{MMCT_2} = \frac{1}{\sqrt{2}}(\lvert a\bar{a}c\bar{c}\rvert - \lvert b\bar{b}c\bar{c}\rvert)$	
$^1\Psi_{LMCT} = \frac{1}{2}(\lvert a\bar{a}c\bar{b}\rvert - \lvert b\bar{a}c\bar{b}\rvert - \lvert a\bar{b}b\bar{c}\rvert + \lvert a\bar{a}b\bar{c}\rvert)$	$\lvert a\bar{a}c\bar{b}\rvert$ $\lvert b\bar{a}c\bar{b}\rvert$ $\lvert a\bar{b}b\bar{c}\rvert$ $\lvert a\bar{a}b\bar{c}\rvert$
$^3\Psi_{LMCT} = \frac{1}{2}(\lvert a\bar{a}c\bar{b}\rvert + \lvert b\bar{a}c\bar{b}\rvert - \lvert a\bar{b}b\bar{c}\rvert - \lvert a\bar{a}b\bar{c}\rvert)$	
$^1\Psi_{DCT} = \lvert a\bar{a}b\bar{b}\rvert$	$\lvert a\bar{a}b\bar{b}\rvert$

[a] Moreover, singlet and triplet states are labeled by their multiplicity, $^1\Psi$ and $^3\Psi$, respectively.

dx.doi.org/10.1021/ic200198f |Inorg. Chem. 2011, 50, 5577–5586

Table 2. Decomposition of the VB Triplet Molecular-Based Covalent Determinants in Terms of the Basic Atomic-Based Determinants Defined in Table 1[a]

	I = $\lvert\Phi_A\bar{\Phi}_B\Phi_C\bar{\Phi}_C\rvert$	II = $\lvert\Phi_B\bar{\Phi}_A\Phi_C\bar{\Phi}_C\rvert$
$\lvert a\bar{b}c\bar{c}\rvert$	$1 - h_{ac}^2/\delta_{ac}^2$	0
$\lvert b\bar{a}c\bar{c}\rvert$	0	$1 - h_{ac}^2/\delta_{ac}^2$
$\lvert a\bar{a}c\bar{c}\rvert$	$\sigma_{AB}/2 + h_{ac}\sigma_{AC}/\delta_{ac} + h_{ac}^2/\delta_{ac}^2$	$\sigma_{AB}/2 + h_{ac}\sigma_{AC}/\delta_{ac} + h_{ac}^2/\delta_{ac}^2$
$\lvert b\bar{b}c\bar{c}\rvert$	$\sigma_{AB}/2 + h_{ac}\sigma_{AC}/\delta_{ac} + h_{ac}^2/\delta_{ac}^2$	$\sigma_{AB}/2 + h_{ac}\sigma_{AC}/\delta_{ac} + h_{ac}^2/\delta_{ac}^2$
$\lvert a\bar{a}c\bar{b}\rvert$	h_{ac}/δ_{ac}	0
$\lvert a\bar{a}b\bar{c}\rvert$	0	h_{ac}/δ_{ac}
$\lvert b\bar{a}c\bar{b}\rvert$	0	$-h_{ac}/\delta_{ac}$
$\lvert a\bar{b}b\bar{c}\rvert$	$-h_{ac}/\delta_{ac}$	0
$\lvert a\bar{a}b\bar{b}\rvert$	$-h_{ac}^2/\delta_{ac}^2$	$-h_{ac}^2/\delta_{ac}^2$

[a] Ground-state singlet and triplet wave functions are constructed by ± combinations of the various terms (eq 18).

MO-CI approach,[26] as well as in the conceptually similar VB-CI approach[22,44] (assuming there $\sigma_{AB} = 0$ and $h_{ab} = 0$, that is, neglecting metal−metal over bridge−metal terms). We already showed above how to extract the parameter h_{ac}/δ_{ac} from the DFT output files (just below eqs 4 and 5). In the present atomic approach, ΔE_{DCT} can be estimated to be larger than δ_{ac} by at least U.[26] Therefore, the magnitude of the DCT contribution to J^{CI} will be mostly damped. The magnitude of J^{CI} can be properly computed by evaluating the values of the various parameters involved: U, δ_{ac} (and h_{ab}), within the framework of (DD)CI codes designed for that effect. We chose to follow here another strategy, consisting of deriving alternative expressions for the exchange coupling constant from a "top-down" point of view, starting from explicit magnetic orbitals. All needed parameters will come directly out of the DFT output files.

Top-Down Derivation. In what follows, we will express VB singlet and triplet states in terms of magnetic and bridge orbitals (eqs 4, 5, and 12). These states will be further expanded in terms of the elementary singlets and triplets constructed from the orthogonalized atomic orbitals $\{a, b, c\}$. This will manifest how these VB-GSs (as well as the VB-BS state for that matter) realize only partial VB-CI expansions. From this "top-down" point of view, these states are formally given by

$$^{1,3}\Psi_{GS} \sim \frac{1}{\sqrt{2}}(\lvert\Phi_A\overline{\Phi}_B\Phi_C\overline{\Phi}_C\rvert \pm \lvert\Phi_B\overline{\Phi}_A\Phi_C\overline{\Phi}_C\rvert) \qquad (18)$$

with the "+" sign for the singlet state ("−" for the triplet, respectively) and the upper bar for β spin. In eq 18, $\{\Phi_A, \Phi_B\}$ stands for the VB magnetic orbitals (eq 4) common to both states. We will further give to the generic VB bridge orbital pair "$\Phi_C\bar{\Phi}_C$" two different forms, depending on whether one starts from triplet (eq 12) or BS (eq 5) bridge orbitals. We therefore derive two alternative expressions J_ω ($\omega = 1, 2$) for the exchange coupling constant (the choice of the indices 1 vs 2 will become clear at the end of the derivation).

(i) Triplet Orbital Based J_2. In this first case, we construct both triplet and singlet states only from the triplet state's magnetic and bridge orbitals (eqs 4 and 12). More explicitly, both the singlet and triplet states (eq 18) are developed in terms of the basic determinants of Table 1. The results of such developments are presented in Table 2. One can then compute their respective energies. In particular, the variational minimization of the singlet-state energy yields the following relation:

$$\Delta_{gu} = -U_2\left(\overline{S} + \frac{h_{ac}^2}{\delta_{ac}^2}\right) = -U_2\overline{S}_2 \qquad (19)$$

where $\overline{S} = \langle\Phi_A^{BS}|\Phi_B^{BS}\rangle$ (eq 6). Plotting $-\Delta_{gu}$ as a function of $\overline{S}_2$ yields an estimate of U_2. Finally, the exchange coupling constant derived from triplet orbitals only is given by

$$J_2 = 2K_{ab} - U_2\left(\overline{S} + \frac{h_{ac}^2}{\delta_{ac}^2}\right)^2 = 2K_{ab} + J_2^{AF} \qquad (20)$$

Notice that J_2 is given here without the additional DCT term because we will compare it with computed J^{BS} values, devoid of DCT contributions. However, in contrast to eq 17, all needed quantities in eqs 19 and 20 can be extracted from the DFT output files. Finally, J_2 could be directly compared to CI-like values, only with the restriction of these being computed at the same "3 sites−4 electrons" level (CAS+1 h+2 h in DDCI nomenclature[26]).

(ii) BS Orbital Based J_1. As an alternative to J_2, we now want to derive an exchange coupling constant based only on the BS magnetic and bridge orbitals. In order to construct triplet and singlet states in which the bridge content is symmetrized, we make use of the "perfect-pairing" (PP) approximation[45−47] by replacing $\lvert\Phi_C\bar{\Phi}_C\rvert$ in eq 18 by $\lvert\Phi_{C_A}\Phi_{C_B}(\alpha\beta - \beta\alpha)\rvert \rightarrow \lvert(\Phi_{C_A}\bar{\Phi}_{C_B} + \Phi_{C_B}\bar{\Phi}_{C_A})\rvert$. It can then be verified in Table 3 that columns I and II, on the one hand, and columns III and IV, on the other hand, provide for different but complementary contributions to the triplet and singlet wave functions developed in terms of the basic determinants of Table 1. This difference is due to the fact that the BS bridge orbitals (cf. eq 5) are lateralized with respect to (a, b) (see Figure 1, right). Consequently, the singlet state derived from the BS state is constructed from Table 3 by summing the contributions of the four columns (I + II + III + IV). The corresponding triplet wave function is constructed from Table 3 as (I − II + III − IV), from which one derives analytical expressions for their respective energies. The variational condition applied to the singlet-state energy now yields

$$\Delta_{gu} - \delta_{ac}m = -U_1\left(\overline{S} - \frac{h_{ac}\sigma_{AC}}{\delta_{ac}}\right) = -U_1\overline{S}_1 \qquad (21)$$

where $m = (h_{ac}/\delta_{ac})(\sigma_{AC} + h_{ac}/\delta_{ac})$ and $\overline{S}$ is given in eq 6. We found numerically that the quantity $\delta_{ac}m$ is nearly constant and will be of very little consequence to the extraction procedure of U_1 (an independent estimation of δ_{ac} is tentatively provided in eq S12 in the Supporting Information). A plot of $-\Delta_{gu}$ as a function of $\overline{S}_1$ yields an estimate of U_1. The exchange coupling constant derived only from BS orbitals is given (without DCT term) by

$$J_1 = 2K_{ab} - U_1\left(\overline{S} - \frac{h_{ac}\sigma_{AC}}{\delta_{ac}}\right)^2 = 2K_{ab} + J_1^{AF} \qquad (22)$$

As it turns out, the two procedures above yielding J_1 and J_2 can be summarized in a very synthetic way. The variational condition applied to each of the two singlet-state energies can be recast into a common shape ($\omega = 1, 2$):

$$\Delta_\omega = -U_\omega\overline{S}_\omega \qquad (23)$$

where $\Delta_\omega = \Delta_{gu} - (2 - \omega)\delta_{ac}m$ and $\overline{S}_\omega = \sigma_{AB} + 2\mu + \omega m$. The original "2 sites−2 electrons" quantities Δ_{gu} and $\overline{S}$ are now

dx.doi.org/10.1021/ic200198f |Inorg. Chem. 2011, 50, 5577–5586

Table 3. Decomposition of the VB-BS Molecular-Based Covalent Determinants in Terms of the Basic Atomic Orbital-Based Determinants Defined in Table 1[a]

	I = $\lvert\Phi_A\bar{\Phi}_B\Phi_{C_A}\bar{\Phi}_{C_B}\rvert$	II = $\lvert\Phi_B\bar{\Phi}_A\Phi_{C_B}\bar{\Phi}_{C_A}\rvert$	III = $\lvert\Phi_A\bar{\Phi}_B\Phi_{C_B}\bar{\Phi}_{C_A}\rvert$	IV = $\lvert\Phi_B\bar{\Phi}_A\Phi_{C_A}\bar{\Phi}_{C_B}\rvert$
$\lvert a\bar{b}c\bar{c}\rvert$	$1-\sigma_{AC}^2$	0	$1-\sigma_{AC}^2-2h_{ac}\sigma_{AC}/\delta_{ac}-2h_{ac}^2/\delta_{ac}^2$	0
$\lvert b\bar{a}c\bar{c}\rvert$	0	$1-\sigma_{AC}^2$	0	$1-\sigma_{AC}^2-2h_{ac}\sigma_{AC}/\delta_{ac}-2h_{ac}^2/\delta_{ac}^2$
$\lvert a\bar{a}c\bar{c}\rvert$	$\sigma_{AB}/2$	$\sigma_{AB}/2$	$\sigma_{AB}/2+h_{ac}\sigma_{AC}/\delta_{ac}+h_{ac}^2/\delta_{ac}^2$	$\sigma_{AB}/2+h_{ac}\sigma_{AC}/\delta_{ac}+h_{ac}^2/\delta_{ac}^2$
$\lvert b\bar{b}c\bar{c}\rvert$	$\sigma_{AB}/2$	$\sigma_{AB}/2$	$\sigma_{AB}/2+h_{ac}\sigma_{AC}/\delta_{ac}+h_{ac}^2/\delta_{ac}^2$	$\sigma_{AB}/2+h_{ac}\sigma_{AC}/\delta_{ac}+h_{ac}^2/\delta_{ac}^2$
$\lvert a\bar{a}c\bar{b}\rvert$	$-\sigma_{AC}$	0	h_{ac}/δ_{ac}	0
$\lvert a\bar{a}b\bar{c}\rvert$	0	$-\sigma_{AC}$	0	h_{ac}/δ_{ac}
$\lvert b\bar{a}c\bar{b}\rvert$	0	σ_{AC}	0	$-h_{ac}/\delta_{ac}$
$\lvert a\bar{b}b\bar{c}\rvert$	σ_{AC}	0	$-h_{ac}/\delta_{ac}$	0
$\lvert a\bar{a}b\bar{b}\rvert$	$-\sigma_{AC}^2$	$-\sigma_{AC}^2$	$-h_{ac}^2/\delta_{ac}^2$	$-h_{ac}^2/\delta_{ac}^2$

[a] Ground-state singlet and triplet wave functions are constructed by ± combinations of the various terms (eq 18).

Table 4. DFT (B3LYP) Parameters and Exchange Coupling Constants for Hydroxo-Bridged Copper(II) Dimers as a Function of the Cu−O−Cu Angle θ (deg)[a]

θ	Δ_{gu} (eV)	$\overline{S}$	h_{ac}/δ_{ac}	σ_{AC}	$\overline{S}_1$	$\overline{S}_2$	J_1^{AF}	J_2^{AF}	J^{BS}	J^{exp}
110.6	0.903	−0.271	0.422	−0.094	−0.231	−0.093	−1963	−392	−1866	−990
108.6	0.842	−0.256	0.415	−0.092	−0.218	−0.084	−1748	−320	−1642	−837
106.6	0.776	−0.240	0.410	−0.091	−0.203	−0.072	−1516	−235	−1405	−684
104.6	0.718	−0.227	0.404	−0.088	−0.191	−0.064	−1342	−186	−1220	−531
102.6	0.657	−0.212	0.399	−0.086	−0.178	−0.053	−1165	−127	−1033	−378
100.6	0.590	−0.197	0.395	−0.084	−0.164	−0.041	−989	−76	−838	−225
98.6	0.532	−0.183	0.390	−0.081	−0.151	−0.031	−839	−44	−687	−72
96.6	0.469	−0.168	0.387	−0.078	−0.138	−0.018	−700	−15	−524	81
94.6	0.415	−0.155	0.382	−0.075	−0.126	−0.009	−584	−4	−401	234
92.6	0.356	−0.141	0.379	−0.071	−0.114	0.003	−478	0	−281	387
90.6	0.301	−0.127	0.376	−0.068	−0.101	0.014	−375	−9	−178	540

[a] J_ω values are given in cm^{-1}, and J_{exp} values are extrapolated from a fit of the experimental data for nearly planar complexes.

corrected within the present "3 sites−4 electrons" derivation by the bridge-only related quantity m and become Δ_ω and $\overline{S}_\omega$, respectively. It is therefore interesting that both sets of formulas (for ω = 1, 2) only differ in the quantification of the bridge content, as expected. Finally, the energy difference between the optimized singlet and triplet gives the exchange coupling constant J_ω:

$$J_\omega = 2K_{ab} - U_\omega \overline{S}_\omega^2 = 2K_{ab} + J_\omega^{AF} \qquad (24)$$

Setting ω = 1 in eqs 23 and 24 yields eqs 21 and 22 (ω = 2 yields eqs 19 and 20). Equation 24 is strongly reminiscent of Noodleman's equation (see item iv in the Introduction). Its form reflects (and we verified it in each case) that the energy of a given BS state is exactly halfway between those of the corresponding triplet and singlet states.

The question now arises as to which (if any) of the two constants J_ω (ω = 1, 2) best describes the magnitude of the DFT−BS-computed J^{BS} coupling.

DFT RESULTS

Methodology. All DFT calculations have been performed with the *ADF 2009* package.[48−53] We use the B3LYP XC potential[54,55] with a triple-ζ basis set throughout. The procedure yielding the VB magnetic orbitals $\{\Phi_A, \Phi_B\}$ has been described in the first paper of the series. The quantity $\overline{S} = \langle\Phi_A^{BS}|\Phi_B^{BS}\rangle$ is computed straightforwardly from the ADF output file as $\overline{S} = \Sigma_i\Sigma_j C_A^i C_B^j \langle\varphi_i|\varphi_j\rangle$ with $\Phi_A^{BS} = \Sigma_i C_A^i \varphi_i$ and $\Phi_B^{BS} = \Sigma_j C_B^j \varphi_j$. Here, $\{\varphi_i\}$ represents the basic Slater atomic orbitals over which the magnetic orbitals are developed. The atomic orbital overlaps $\sigma_{AC} = \langle A|C\rangle$ (A = "d" for the Cu^{II} ion and C = "p" for the symmetry-adapted bridge orbital) as well as the ratio c_C/c_A of their respective coefficients in the NO-VB magnetic orbital $\Phi_A \approx c_C C + c_A A$ (+ other terms ...) are directly extracted from the ADF triplet and BS output files. Homemade codes have been written to extract all needed parameters.

Copper(II) Dimers. *Examples Suited for the "3 Sites−4 Electrons" Model.* All of the data pertaining to analysis of the ideally symmetrized and planar hydroxo-bridged copper(II) dimer $[Cu_2(OH)_2(NH_3)_4]^{2+}$ are reported in Table 4. The Cu−O distance is kept constant at 1.977 Å as is the Cu−N distance (2.020 Å). We only vary the Cu−O−Cu angle θ. Equivalent data are reported in the Supporting Information for azido- (section B1), methoxo- (section B2), and aquo-bridged (section B3) species.

We first plot Δ_ω values for the hydroxocopper dimer as a function of $\overline{S}_\omega$ (see eqs 19, 21, and 23 and Figure S6 in the Supporting Information), which yields U_1 = 4.56 eV and U_2 = 5.62 eV. We then report these values in the corresponding eqs 20, 22, and 24 to estimate the antiferromagnetic part of J_ω and plot it *without further adjustment* against the DFT-computed J^{BS} values (Figure 2; the equivalent figure combining all of the plots pertaining to the four idealized copper dimers studied in the

dx.doi.org/10.1021/ic200198f |*Inorg. Chem.* 2011, 50, 5577–5586

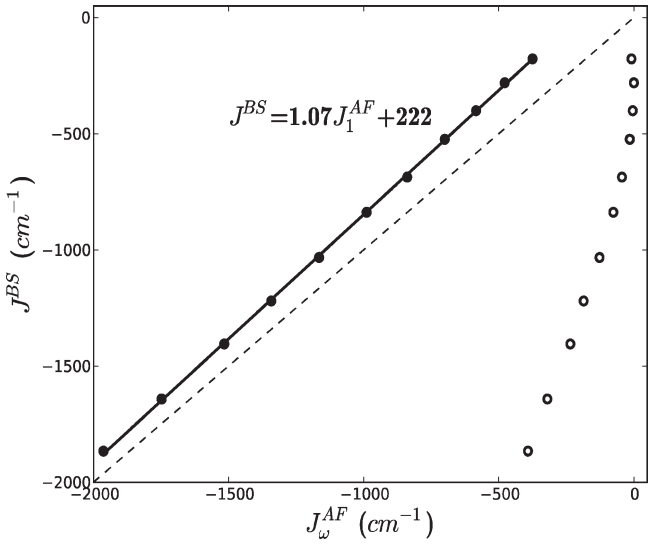

Figure 2. BS exchange coupling constant J^{BS} as a function of the antiferromagnetic part of J_ω^{AF} (filled circles for $\omega = 1$ and empty circles for $\omega = 2$). The dashed line corresponds to the identity $J^{BS} = J_\omega^{AF}$.

present work is reported in Figure S7 in the Supporting Information).

(i) For $\omega = 1$, the slope is close enough to unity (1.07) and the intercept of 222 cm^{-1} is interpreted as the ferromagnetic $2K_{ab}$ contribution. Notice that these ("3 sites−4 electrons") values of U_1 and $2K_{ab}$ are close to those reported in the first paper of the series within a "2 sites−2 electrons" framework where U^{eff} was, however, only an effective fit parameter resulting from $J^{BS} = f(\overline{S^2})$.

(ii) For $\omega = 2$, the J_2^{AF} values versus J^{BS} are very different and the amplitude of variation of J_2 is much smaller than that of J^{BS}. Simply put, Figure 2 shows that J_1 reproduces the J^{BS} values, whereas J_2 does not. Following the same procedure, we calculated U_ω and J_ω values for various ideally symmetric copper(II) dimer bridges $[Cu_2(X)_2(NH_3)_4]^{n+}$. In Table 5, values for U_1, U_2, $2K_{ab}$, and the slopes are reported (the case of the chloro-bridged dimer will be discussed in the Appendix).

To this collection, we also added a "real" copper(II) dimer,[56] $[CuL(H_2O)]_2 2H_2O$, bridged by L = *N*-picolinoyl-3-amino-1-propanol (papen; see Figure 3). Its Cu−O−Cu angle value is 98.3°, and the exchange coupling constant measured experimentally for this hydrated compound is −128 cm^{-1}, although that value is not derived from a binuclear formulation of the magnetic susceptibility but from an approximate tetrameric ring formulation. When starting from such a "real" system, the strategy consists of drawing a limited magnetostructural correlation in order to get U_ω values (DFT data in section B4 in the Supporting Information). Starting from the X-ray crystallographic geometry, we generated four additional geometries by moving both Cu atoms symmetrically along the Cu−Cu axis, bringing them further away from, and closer to, one another (step: 0.05 Å). In this case, U_1 = 1.54 eV and U_2 = 1.73 eV. Plotting J^{BS} as a function of J_1 yields a slope of 1.17 and an intercept value $2K_{ab}$ of 174 cm^{-1}. Notice that both U_ω values are smaller for this real dimer than for the corresponding methoxo-idealized one because of the additional expansion of the magnetic orbital toward the pyridine ring in the former case (Figure 3). Next, we can compare

Table 5. Parameters Derived for Various Copper(II) Dimers at the B3LYP Level (See Figures 2 and S1−S5 in the Supporting Information for Fits and Tables S1−S5 in the Supporting Information for DFT Data)[a]

bridge	U_1 (eV)	slopes	$2K_{ab}$ (cm^{-1})	U_2 (eV)
hydroxo	4.56	1.07	222	5.62
azido	3.84	1.05	878	4.21
methoxo	4.44	1.00	378	6.08
aquo	4.34	1.15	28	4.32
papen	1.54	1.17	174	1.73
chloro	6.56	0.86	818	2.01

[a] Slopes are extracted from the fit of J_{BS} as a function of J_1^{AF}.

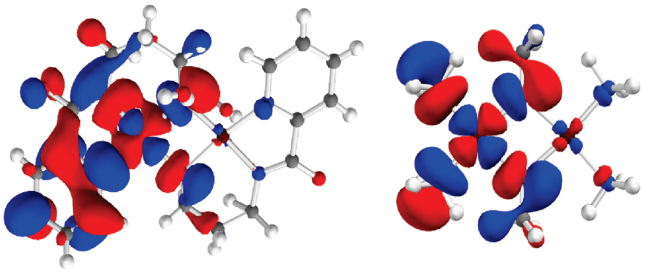

Figure 3. Representation of the (β-spin-unrestricted) LUMOs mirroring the SOMOs for the "real" papen (left) and idealized methoxo (right) copper dimers (B3LYP). The isosurface value is set to 0.02 au.

the computed J^{BS} value of the original geometry (−424 cm^{-1}) with that measured experimentally: −128 cm^{-1}. A rough reduction factor of 2 applied to J^{BS} would bring the computed value closer to the experimental one. Finally, for a Cu−O−Cu angle of 98.3°, the extrapolation of the magnetostructural correlation curve (cf. the first paper of the series) for experimental (nearly planar) alkoxo-bridged copper(II) dimers predicts a ferromagnetic exchange coupling constant of 248 cm^{-1}. The difference between the measured (−128 cm^{-1}) and extrapolated (248 cm^{-1}) values is not due to the presence of the water molecules because the anhydrous version of the papen-bridged copper dimer (all other structural data being conserved) yields J^{BS} = −441 cm^{-1}. This illustrates the sensitivity of the measured or computed exchange coupling constants to the geometries of the complexes (here, nearly planar versus distorted papen). To conclude this section about copper(II) dimers, in all of these cases, we found that only the analytical J_1 constant constructed from the BS MOs satisfyingly reproduces the magnetostructural features of the corresponding DFT-computed J^{BS} values.

DISCUSSION

In the previous sections, we derived two analytical expressions for the exchange coupling constant J_ω (eqs 20, 22, and 24 with $\omega = 1, 2$). J_1 is obtained by expressing triplet- and singlet-state wave functions and energies from DFT−BS orbitals only (cf. Figure 1, right). For that, we used the PP method for the bridge. By contrast, J_2 results from the sole use of the triplet state, magnetic and bridge mutually orthogonal orbitals (Figure.1, left). Notice that, in both cases, the same NO-VB magnetic orbitals enter in eq 18. The source of the difference between J_1 and J_2 lies, therefore, only in the description of the bridge. However, both J_1 and J_2 differ from J^{CI} (eq 17) in that they both

dx.doi.org/10.1021/ic200198f |*Inorg. Chem.* 2011, 50, 5577–5586

(in their own way) realize *partial* atomic CI expansions, whereas J^{CI} is derived from a *full* CI expansion via the matrix in eq 14. Finally, a computed DFT−BS value $J^{BS} = 2(E_{BS} - E_T)$ is conceptually hybrid in the sense that both DFT triplet and BS state energies differ not only because of physically sound LMCT/MMCT mechanisms but mainly because of an unphysical symmetry breaking of the bridge orbitals inherent to the unrestricted DFT−BS methodology. Therefore, J^{BS} is not strictly speaking an exchange coupling constant.

Computed J_{BS} Values Reproduced by J_1. The analytical expression of J_1 explicitly contains LMCT and MMCT contributions but neither DCT nor intra/interspin-polarization terms. In addition to such quantities defined in the first paper of the series as the intersite delocalization parameter μ and the DFT−BS magnetic overlap $\overline{S}$, we extracted from DFT calculations specific parameters (ratio h_{ac}/δ_{ac} and atomic orbital overlaps σ_{AB} and σ_{AC}) suitable for our "3 sites−4 electrons". By applying our analytical model to various copper dimers, we verified that, in each case, J_1 reproduces correctly the variation of J^{BS} (slope close to unity). We, therefore, validate a posteriori the minimal physics required by the BS methodology.[2] Moreover, plotting J^{BS} as a function of J_1^{AF} yields the intercept values reported in Table 5, which are interpreted as the residual ferromagnetic constant $2K_{ab}$.

We further verified that the agreement between J_1 and J^{BS} does not depend on the percentage of HF exchange mixed into the XC potential. It can be seen in Figure S8 in the Supporting Information (see also Tables S8 and S9 in the Supporting Information) drawn for the hydroxo-bridged copper(II) dimer that, from 20% to 50% HF, the slopes remain close to unity. Moreover, as can be expected, the $2K_{ab}$ estimations decrease with an increase in the percent of HF as the magnetic orbitals retreat toward the copper sites.

J_2 as a First Step toward Experimental Values. The expression of J_2 contains the same physics as that of J_1 (i.e., LMCT and MMCT), but it is developed on a different (triplet bridge) orbital basis. The magnitude of J_2 is much smaller than that of $J_1 \approx J^{BS}$. This means that the energy of the singlet state estimated from the DFT triplet-state orbitals and yielding J_2 is higher than that of the singlet state corresponding to J_1 and derived from BS orbitals. This is most probably related to the fact that, in the computed BS state, the breaking of the bridge symmetry offers an additional degree of liberty (with respect to the triplet state), leading to an extra stabilization of the BS state. The comparison between CI-calculated J values using either triplet or singlet MOs has been reported in the literature.[35] The values are somewhat different at the CAS-CI level but much less contrasted than the differences reported here between J_1 and J_2. This shows more that the difference between J_1 and J_2 is not mechanistic, as Noodleman's BS formalism is physically sound, but is artificially caused by the unrestricted DFT−BS methodology.

Numerically, we expect the magnitude of J_2 to be closer to those computed at the CAS+S level. In effect, post-self-consistent-field (SCF) CAS calculations start from the triplet state's orbitals, as does J_2 in our derivation. Therefore, were the DFT orbitals suited for such a purpose, J_2 would constitute the first term to which other post-DFT contributions (DCT, intra/interligand spin polarization, etc.) could be added by perturbation in order to (hopefully) reach experimental values. In this way, from our "top-down" approach, we derive an analytical expression of the DCT contribution $-8h_{ac}^4/\delta^3(1 - \Delta E_{DCT}/4\delta_{ac})$ to be added to J_2. This last expression shows a crucial dependence in the ratio $\Delta E_{DCT}/4\delta_{ac}$. However, we do not yet have a clear-cut procedure to evaluate the ΔE_{DCT} quantity as well as δ_{ac} (see, however, eq S12 in the Supporting Information).

There are still conceptual differences between our approach yielding J_2 and CAS or post-CAS (i.e., DDCI) procedures. In effect, we expressed all NO-VB orbitals (eqs 4, 5, and 10−12) and basic singlets (Table 1) in terms of orthogonalized *atomic* orbitals $\{a, b, c\}$ (our building bricks). As a consequence, the physical content of J_2 is explicitly built at the atomic orbital level and, therefore, resembles other VB-CI approaches,[22,44] where, for example, atomic-based DCT terms appear explicitly. By contrast, in the minimal "active space" of a DDCI calculation, all interatomic charge-transfer contributions definable for a given active space are implicitly taken into account during the SCF calculation, yielding the triplet (or singlet) state. This procedure yields magnetic (antibonding) and corresponding bridge (bonding) orbitals, which, in turn, become the elementary bricks of subsequent post-SCF perturbation contributions. As a consequence, the residual orbital-based DCT contributions (called "2 h" in Malrieu et al.'s terminology) resulting from other bridge orbitals are expected to be small due to Brillouin's theorem.[26]

Finally, the CAS/DDCI methods developed by Malrieu et al. do a very fine job in reproducing experimental values, and we do not see yet how to rival such theories with our DFT tools because (to start with) of the intrinsic limitations of the BS methodology listed in the Introduction. As a consequence, the focus of the present work was rather to give an analytical expression to J^{BS} within the minimal "3 sites−4 electrons" framework, opening the way for a better understanding of the physics involved in an actual DFT−BS calculation.

CONCLUSIONS

Despite its apparent conceptual deficiencies, the BS methodology is still surprisingly robust and convenient to reproduce experimental trends and to yield insights into some of the exchange mechanisms involved in the process, especially basic and fundamental MMCT and LMCT terms. It has to remain clear, however, that the BS state, constructed as it is from NO-VB orbitals, when expanded into orthogonalized (atomic or molecular) orbitals in a "top-down" procedure (eq 18), realizes only a partial CI optimization. By contrast, the "bottom-up" approach (eq 14) provides a full CI expansion for both the triplet and singlet states.

Usually, a BS state is thought as resulting from the symmetry breaking of the magnetic orbitals. We showed, however, in the present work that the bridge orbital symmetry of the triplet state (eqs 9 and 12) is artificially broken in the BS state (eqs 2 and 5). As a consequence, the DFT-computed J^{BS} is not stricto sensu an exchange coupling constant because the BS state does not exhibit physically sound bridge orbitals (cf. Figure 1). To the best of our knowledge, it is the first time that the symmetry breaking of the bridge orbitals is shown to have such an impact on the magnitude of J^{BS}. This effect, therefore, contributes to the overestimation of J^{BS} compared to experimental values, in addition to other effects already mentioned.

We showed, however, that it is still possible to derive a highly significant analytical expression J_1 (eq 22) numerically matching the DFT-computed J^{BS} for various copper(II) dimers suitable for a NO-VB description. The linear fits of J^{BS} as a function of J_1^{AF} work with slopes near 1 and ferromagnetic terms as intercepts for

dx.doi.org/10.1021/ic200198f |*Inorg. Chem.* 2011, 50, 5577–5586

several systems over a range of bridge geometries (angles), moreover using different DFT hybrid functions from 20% to 50% HF mixtures. We thus now have a fair idea of what J^{BS} means in terms of a VB-CI expansion. The corresponding true exchange coupling constant J_1 has been constructed only from the DFT−BS state using the same magnetic and bridge orbital basis. However, by construction, J_1 incorporates the same defect as J^{BS} at the level of the bridge.

One may still think that the problem at stake, that is the fact that the unrestricted DFT−BS method yields exchange coupling constants of usually too large magnitude, is more with finding the physically correct DFT than with the BS method itself. On the one hand, some authors[57,58] have remarked that the BS state can be seen as an artifact whose existence is due to our lack of knowledge of the exact XC potential. Were this exact XC potential known, the BS state would either not exist or be at best an excited state (i.e., the ground state would be the true singlet state for antiferromagnetic systems). On the other hand, for a given (as of yet approximate) XC potential and resulting BS state, there is a basic difference between the BS state, as it is described from a formal point of view,[1,2] and the actual unrestricted DFT−BS state, as it comes out of a calculation. That difference lies at the level of the bridge orbitals and has a large impact on computed J^{BS} values. As of yet, we do not see a way around that defect in the unrestricted DFT−BS methodology itself. We still hope that our analysis represents a good start toward further progress.

From a pragmatic point of view, it seems that the combined use of the B3LYP XC potential with an empirical reduction factor of 2 of the magnitude of $J_1 \approx J^{BS}$ works just fine for a wide range of spin-coupled copper(II) complexes.[27] The source of this drastic measure is supposedly linked to the so-called SIE, that is the nonexact compensation between (exact) Coulombic and (approximate) exchange energies designed to remove the electron self-interaction energy.[57,58] The tools we developed in the present paper (especially J_1 versus J_2) will allow us to distinguish between pure DFT (i.e., SIE) and BS methodology (i.e., bridge) problems (manuscript in preparation).

Concerning our expression J_2 (eq 20; possibly with some DCT contribution), we have applied it to ideally symmetrical (C_{2v}) and chemically simple (NH_3 terminal ligands) copper dimers (cf. Table 4 and sections B1−B3 in the Supporting Information). These values cannot be compared directly to those derived from experimental correlations drawn for realistic complexes exhibiting lower symmetries and richer chemistry (the case of the papen copper dimer treated above). It would be necessary to compare numerically our J_2 values with CAS(+1 h+2 h)/CAS+S values for the same set of ideal systems and, ultimately, with DDCI values. This part is already in progress through a collaboration.

APPENDIX: EXTENSION OF THE FORMALISM

In the previous formalism, we only considered one bridge *c* orbital belonging to the *gerade* SOMO symmetry in order to keep the derivations as simple as possible. By the generic term "*c*", we meant the symmetry-adapted linear combination of bridge (s and p) atomic orbitals interacting with the "+" combination of copper ninth d orbitals yielding the *gerade* triplet SOMO. It is possible, however, to treat in the very same way the other *ungerade* SOMO symmetry. The generic bridge orbital will be labeled "*d*". We give here only a few key expressions derived at

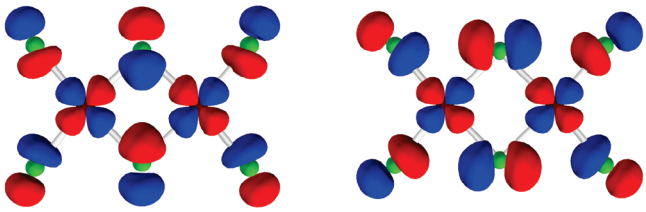

Figure 4. Representation of the two (β-spin-unrestricted) LUMOs mirroring the two SOMOs for a $[Cu_2Cl_6]^{2-}$ dimer computed with B3LYP. The isosurface value is set to 0.04 au, and the bridge angle [Cu−Cl−Cu] is 89°.

what we now call the "3 sites−6 electrons" level. Some details of the derivation are furnished as section A4 in the Supporting Information. The DFT−BS magnetic orbital overlap $\overline{S}$ is now expressed to the second order as (cf. eq 6)

$$\overline{S} = \sigma_{AB} + 2\mu + \left(\frac{2h_{ac}\sigma_{AC}}{\delta_{ac}} + \frac{{h_{ac}}^2}{{\delta_{ac}}^2}\right) - \left(\frac{2h_{ad}\sigma_{AD}}{\delta_{ad}} + \frac{{h_{ad}}^2}{{\delta_{ad}}^2}\right) \tag{25}$$

and the triplet SOMO gap Δ_{gu} becomes (cf. eq 13)

$$\Delta_{gu} = 2h_{ab} + \frac{2{h_{ac}}^2}{\delta_{ac}} - \frac{2{h_{ad}}^2}{\delta_{ad}} \tag{26}$$

For both symmetries, the product $h\sigma < 0$ and setting aside $h_{ab} \leftrightarrow \sigma_{AB} + 2\mu$ in eqs 25 and 26, we verify that both $\overline{S}$ and Δ_{gu} cancel when *c* and *d* weigh equivalently in the two magnetic orbitals. These analytical "3 sites−6 electrons" expressions are relevant for a proper description of the exchange phenomenon within, for example, copper(II) dimers bridged by μ-chloro moieties. We tested this last model and show in Figure 4 a representation of the two triplet SOMOs, each selecting the corresponding symmetry-adapted bridge orbitals: the $3p_y$ (+3s) chloride orbital interacts with the metallic ($d_a - d_b$) combination and the $3p_z$ orbital with the ($d_a + d_b$) combination.

We derived the appropriate formula for the exchange coupling constants: in Δ_ω (cf. eq 23), $\delta_{ac}m$ is replaced by ($\delta_{ac}m_{ac} - \delta_{ad}m_{ad}$), while in $\overline{S}_\omega$, *m* is replaced by $m_{ac} - m_{ad}$. The form of eq 24 is, however, left unchanged. All needed data are given in section B5 in the Supporting Information. As for the chloro-bridged copper(II) dimers, J_1 fairly reproduces J^{BS} (slope of 0.85), whereas J_2 does not. In the first case, the numerical agreement is not perfect because of the fact that it is more difficult to quantify the result of the difference between *z* and *y* partially compensating terms. Moreover, while the chlorine $3p_z$ orbital is almost the sole contributor to the *gerade* SOMO, such is not the case within the *ungerade* symmetry, containing a mixture of chlorine 3s and $3p_y$ orbitals. A proper analytical treatment of such a mixture turned out to be too cumbersome, even after predefining such a mixture in the DFT calculations via a fragment approach, as is possible with ADF. We therefore did not pursue such a course. Still, J_1 is much closer to J^{BS} than J_2, which is what we wanted to show.

ASSOCIATED CONTENT

Supporting Information. Supplements to the theoretical formalism, DFT results for copper dimers, and miscellaneous

dx.doi.org/10.1021/ic200198f |*Inorg. Chem.* 2011, 50, 5577–5586

results. This material is available free of charge via the Internet at http://pubs.acs.org.

AUTHOR INFORMATION

Corresponding Author

*E-mail: nicolas.onofrio@cea.fr (N.O.), jean-marie.mouesca@cea.fr (J.-M.M.).

REFERENCES

(1) Noodleman, L. *J. Chem. Phys.* **1981**, *74*, 5737–5743.
(2) Noodleman, L.; Davidson, E. *Chem. Phys.* **1986**, *109*, 131–143.
(3) Noodleman, L.; Case, D. *Adv. Inorg. Chem.* **1992**, *38*, 423–458.
(4) Hart, J.; Rappé, A.; Gorun, S.; Upton, T. *J. Phys. Chem.* **1992**, *96*, 6264–6269.
(5) Ciofini, I.; Daul, C. *Coord. Chem. Rev.* **2003**, *238*, 187–209.
(6) Soda, T.; Kitagawa, Y.; Onishi, T.; Takano, Y.; Shigeta, Y.; Nagao, H.; Yoshioka, Y.; Yamaguchi, K. *Chem. Phys. Lett.* **2000**, *319*, 223–230.
(7) Caballol, R.; Castell, O.; Illas, F.; Moreira, P.; Malrieu, J. *J. Phys. Chem. A* **1997**, *101*, 7860–7866.
(8) Neese, F. *Coord. Chem. Rev.* **2009**, *253*, 526–563.
(9) Onofrio, N.; Mouesca, J.-M. *J. Phys. Chem. A* **2010**, *114*, 6149–6156.
(10) Ruiz, E.; Cano, J.; Alvarez, S.; Alemany, P. *J. Am. Chem. Soc.* **1998**, *120*, 11122–11129.
(11) Rodriguez-Fortea, A.; Alemany, P.; Alvarez, S.; Ruiz, E. *Inorg. Chem.* **2002**, *41*, 3769–3778.
(12) Triki, S.; Gomez-Garcia, C.; Ruiz, E.; Sala-Pala, J. *Inorg. Chem.* **2005**, *44*, 5501–5508.
(13) Blanchet-Boiteux, C.; Mouesca, J. *J. Am. Chem. Soc.* **2000**, *122*, 861–869.
(14) Blanchet-Boiteux, C.; Mouesca, J. *J. Phys. Chem. A* **2000**, *104*, 2091–2097.
(15) Hu, H.; Zhang, D.; Liu, Y.; Liu, C. *Chem. Phys. Lett.* **2001**, *340*, 370–375.
(16) Bencini, A.; Totti, F. *Int. J. Quantum Chem.* **2005**, *101*, 819–825.10th International Conference on the Applications of Density Functional Theory in Chemistry and Physics, Brussels, Belgium, Sept 5−12, 2003.
(17) Li, L.; Liao, D.; Jiang, Z.; Mouesca, J.-M.; Rey, P. *Inorg. Chem.* **2006**, *45*, 7665–7670.
(18) Desplanches, C.; Ruiz, E.; Rodriguez-Fortea, A.; Alvarez, S. *J. Am. Chem. Soc.* **2002**, *124*, 5197–5205.
(19) Monari, A.; Maynau, D.; Malrieu, J.-P. *J. Chem. Phys.* **2010**, *133*, 044106.
(20) Zaanen, J.; Sawatzky, G. *Can. J. Phys.* **1987**, *65*, 1262–1271.
(21) Shen, Z.; Allen, J.; Yeh, J.; Kang, J.; Ellis, W.; Spicer, W.; Lindau, I.; Maple, M.; Dalichaouch, Y.; Torikachvili, M.; Sun, J.; Geballe, T. *Phys. Rev. B* **1987**, *36*, 8414–8428.
(22) Tuczek, F.; Solomon, E. *Inorg. Chem.* **1993**, *32*, 2850–2862.
(23) Eskes, H.; Jefferson, J. *Phys. Rev. B* **1993**, *48*, 9788–9798.
(24) Suaud, N.; Lepetit, M. *Phys. Rev. B* **2000**, *62*, 402–409.
(25) Weihe, H.; Gudel, H.; Toftlund, H. *Inorg. Chem.* **2000**, *39*, 1351–1362.
(26) Calzado, C.; Cabrero, J.; Malrieu, J.; Caballol, R. *J. Chem. Phys.* **2002**, *116*, 2728–2747.
(27) Ruiz, E.; Alvarez, S.; Cano, J.; Polo, V. *J. Chem. Phys.* **2005**, *123*, 164110.
(28) Adamo, C.; Barone, V.; Bencini, A.; Broer, R.; Filatov, M.; Harrison, N.; Illas, F.; Malrieu, J.; Moreira, I. *J. Chem. Phys.* **2006**, *124*, 107101.
(29) Ruiz, E.; Cano, J.; Alvarez, S.; Polo, V. *J. Chem. Phys.* **2006**, *124*, 107102.
(30) van Oosten, A.; Broer, R.; Nieuwpoort, W. *Chem. Phys. Lett.* **1996**, *257*, 207–212.
(31) Ruiz, E.; Cano, J.; Alvarez, S.; Alemany, P. *J. Comput. Chem.* **1999**, *20*, 1391–1400.
(32) Cabrero, J.; Calzado, C.; Maynau, D.; Caballol, R.; Malrieu, J. *J. Phys. Chem. A* **2002**, *106*, 8146–8155.
(33) Neese, F. *J. Phys. Chem. Solids* **2004**, *65*, 781–785.Spring Meeting of the European Materials Research Society (EMRS), Strasbourg, France, June 10−13, 2003.
(34) Calzado, C.; Cabrero, J.; Malrieu, J.; Caballol, R. *J. Chem. Phys.* **2002**, *116*, 3985–4000.
(35) Calzado, C. J.; Angeli, C.; Taratiel, D.; Caballol, R.; Malrieu, J.-P. *J. Chem. Phys.* **2009**, *131*, 044327.
(36) Miralles, J.; Castell, O.; Caballol, R.; Malrieu, J. *Chem. Phys.* **1993**, *172*, 33–43.
(37) Calzado, C. sJ.; Angeli, C.; Caballol, R.; Malrieu, J.-P. *Theor. Chem. Acc.* **2010**, *126*, 185–196.
(38) Kahn, O.; Briat, B. *J. Chem. Soc., Faraday Trans. II* **1976**, *72*, 268–281.
(39) Girerd, J.; Journaux, Y.; Kahn, O. *Chem. Phys. Lett.* **1981**, *82*, 534–538.
(40) Kahn, O. *Molecular Magnetism*; VCH Publishers: New York, 1993.
(41) Mouesca, J. *J. Chem. Phys.* **2000**, *113*, 10505–10511.
(42) Albright, T. A.; Burdett, J. K.; Whangbo, M. H. *Orbital Interactions in chemistry*; John Wiley & Sons: New York, 1985.
(43) Hay, P.; Thibeault, J.; Hoffmann, R. *J. Am. Chem. Soc.* **1975**, *97*, 4884–4899.
(44) Tuczek, F.; Solomon, E. *J. Am. Chem. Soc.* **1994**, *116*, 6916–6924.
(45) Hunt, W.; Hay, P.; Goddard, W. *J. Chem. Phys.* **1972**, *57*, 738–748.
(46) Schultz, P.; Messmer, R. *J. Am. Chem. Soc.* **1993**, *115*, 10938–10942.
(47) Voorhis, T.; Head-Gordon, M. *J. Chem. Phys.* **2000**, *112*, 5633–5638.
(48) Baerends, E. J.; Ellis, D. E.; Ros, P. *Chem. Phys.* **1973**, *2*, 41–51.
(49) Baerends, E. J.; Ros, P. *Chem. Phys.* **1973**, *2*, 52–59.
(50) Baerends, E.; Ros, P. *Int. J. Quantum Chem.* **1978**, *12*, 169–190.
(51) Bickelhaupt, F.; Baerends, E.; Ravenek, W. *Inorg. Chem.* **1990**, *29*, 350–354.
(52) Ziegler, T. *Chem. Rev.* **1991**, *91*, 651–667.
(53) Velde, G.; Baerends, E. *J. Comput. Phys.* **1992**, *99*, 84–98.
(54) Lee, C.; Yang, W.; Parr, R. *Phys. Rev. B* **1988**, *37*, 785–789.
(55) Becke, A. *J. Chem. Phys.* **1993**, *98*, 1372–1377.
(56) Bertrand, J.; Fujita, E.; Eller, P. *Inorg. Chem.* **1974**, *13*, 2067–2071.
(57) Cremer, D. *Mol. Phys.* **2001**, *99*, 1899–1940.
(58) Rudra, I.; Wu, Q.; Van Voorhis, T. *J. Chem. Phys.* **2006**, *124*, 024103.